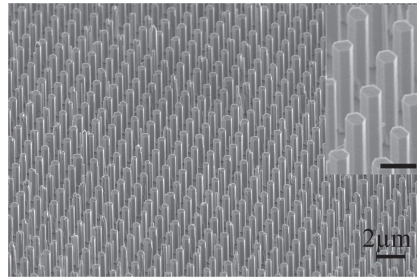


FULL PAPER

Nanowires

D. Yuan, R. Guo, Y. Wei, W. Wu,
Y. Ding, Z. L. Wang,* S. Das*.....x-xx

Heteroepitaxial Patterned Growth of Vertically Aligned and Periodically Distributed ZnO Nanowires on GaN Using Laser Interference Ablation



The figure shows a scanning electron microscope image of vertically aligned ZnO nanowire arrays produced through heteroepitaxial growth on GaN substrates patterned through laser interference ablation. The micrograph shows 45° tilted views of aligned individual ZnO nanowires with uniform diameter, height, and 2 μm period on a portion of a growth area spanning one square centimeter. The inset image is an enlarged view of the nanowires (scale bar is 1 μm).

Heteroepitaxial Patterned Growth of Vertically Aligned and Periodically Distributed ZnO Nanowires on GaN Using Laser Interference Ablation

By Dajun Yuan, Rui Guo, Yaguang Wei, Wenzhuo Wu, Yong Ding, Zhong Lin Wang,* and Suman Das*

A simple two-step method of fabricating vertically aligned and periodically distributed ZnO nanowires on gallium nitride (GaN) substrates is described. The method combines laser interference ablation (LIA) and low temperature hydrothermal decomposition. The ZnO nanowires grow heteroepitaxially on unablated regions of GaN over areas spanning 1 cm², with a high degree of control over size, orientation, uniformity, and periodicity. High resolution transmission electron microscopy and scanning electron microscopy are utilized to study the structural characteristics of the LIA-patterned GaN substrate in detail. These studies reveal the possible mechanism for the preferential, site-selective growth of the ZnO nanowires. The method demonstrates high application potential for wafer-scale integration into sensor arrays, piezoelectric devices, and optoelectronic devices.

1. Introduction

ZnO nanostructures such as nanobelts,^[1] nanowires,^[2] nanorods,^[3] and nanosprings/nanorings^[4] have attracted considerable research interest due to their unique electrical and optical properties for applications in nanogenerators,^[5,6] sensors,^[7] solar cells,^[8] UV lasers,^[9] field emission devices,^[10,11] light emitting diodes,^[12] and logical circuit devices.^[13] Typically sapphire, gallium nitride (GaN) and silicon carbide (SiC) are the commonly used epitaxy substrates for growing ZnO nanowires. GaN and ZnO have similar fundamental bandgap energy (3.37 eV for ZnO, 3.4 eV for GaN), the same wurtzite crystal symmetry, and a low mismatch of the lattice constant (1.9%). These characteristics make conductive high quality n/p-doped GaN a good candidate substrate for ZnO nanowires growth and further applications.^[6]

In recent years, a number of approaches have demonstrated successful large-scale fabrication of nanowire arrays. Electron

beam lithography (EBL) has been demonstrated for the fabrication of aligned ZnO nanowire arrays.^[14] However, EBL is too costly and complex for large-scale production. Nanosphere lithography (NSL)^[3,15,16] and nanoimprint lithography (NIL)^[17,18] are two popular methods to obtain ordered metal catalyst dots for subsequent growth of nanowires. However, in fabricating defect-free and period-adjustable large-area nanowire patterns, these techniques suffer from poor repeatability and limited flexibility. Laser interference lithography (LIL) is known as a reliable and fast technique to achieve large-area periodic patterns.^[19] We recently demonstrated the wafer-scale growth of ZnO nanowire

arrays through LIL of SU-8 photoresist coated on GaN followed by hydrothermal decomposition.^[20] However, to further reduce the cost of patterned nanowire growth processes and to minimize defects, it is highly desirable to employ techniques that combine reliable and reproducible single-step direct patterning of growth substrates with catalyst-free nanowire growth.

In this paper, we demonstrate a simple and efficient two-step approach for the growth of arrays of individual ZnO nanowires, which combines pulsed laser interference ablation (LIA) and hydrothermal decomposition method. Pulsed LIA has the advantages of LIL in the creation of periodic patterns, but more importantly, it can directly produce patterns on GaN substrates, thereby eliminating several process steps compared to the LIL-based approach. The low temperature hydrothermal decomposition method grows ZnO nanowires heteroepitaxially on patterned GaN, without needing catalyst. By combining these techniques, vertically aligned and periodically distributed individual ZnO nanowires can be grown over large areas simply through two steps: patterning and growth. Experimental results show that both the positions and the sizes of the ZnO nanowires can be precisely controlled via the LIA and hydrothermal growth steps.

2. Experimental Design

GaN films, grown on sapphire substrates by metal-organic chemical vapor deposition (MOCVD), were used as the starting materials. **Figure 1** shows fabrication sequences of individual ZnO nanowire arrays. First, the GaN surfaces were structured

[*] Dr. D. Yuan, Dr. R. Guo, Prof. S. Das
Woodruff School of Mechanical Engineering
Georgia Institute of Technology
Atlanta, GA 30332-0405 (USA)
E-mail: sumandas@gatech.edu

Dr. Y. Wei, Mr. W. Wu, Dr. Y. Ding, Prof. Z. L. Wang
School of Materials Science and Engineering
Georgia Institute of Technology
Atlanta, GA 30332-0245 (USA)
E-mail: zhong.wang@mse.gatech.edu

DOI: 10.1002/adfm.201001058

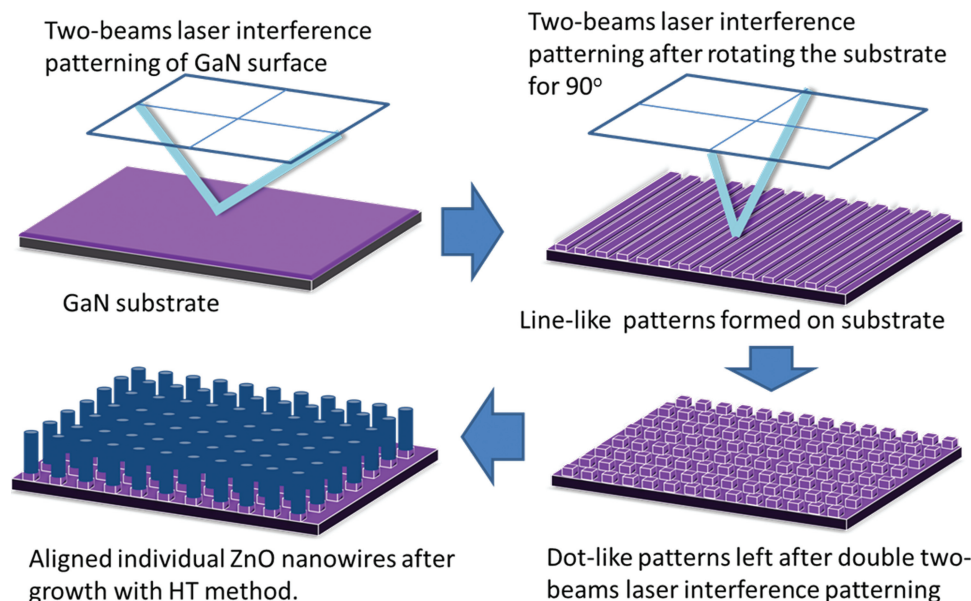


Figure 1. Fabrication sequences of individual ZnO nanowire arrays. GaN substrates were patterned with two-beam LIA to obtain line-like patterns on the surface. The samples were rotated 90° and patterned again to achieve dot-like patterns. The hydrothermal method was then utilized to grow individual ZnO nanowires on the flat mesas area.

by two-beam laser interference patterning to achieve line-like patterns on the surface. Then, the first step was repeated after rotating the substrates by 90 degrees to achieve the isolated mesas. The isolated mesas are actually unablated areas serving as sites for ZnO nanowire growth. Their size and periodicity are controlled by the laser fluence and the angle between the interfering laser beams. A low temperature hydrothermal method was then used to achieve patterned and aligned growth of ZnO nanowires at temperatures below 100 °C on the patterned GaN substrates, without using a catalyst. The low temperature hydrothermal method^[21,22] exhibits tremendous advantages compared to the high temperature vapor deposition method^[23,24] including: low cost, high yield, easy scale-up capability, and polymer compatibility.

3. Results and Discussion

The interference of the beams results in a periodic intensity distribution on the substrate, which is generally described by the equation:

$$F(x) = 2F_0 \left[1 + \cos \left(\frac{4\pi \sin(\frac{\theta}{2})}{\lambda} x + \Delta\phi \right) \right] \quad (1)$$

where F_0 is the intensity of each wave, λ is the wavelength, and $\Delta\phi$ is the phase difference between the two waves. The interference period (P) is determined by the wavelength (λ) and the angle (θ), and is given by the equation $P = \lambda/2 \sin(\theta/2)$.

Figure 2 shows the scanning electron microscopy (SEM) images (LEO 1550) after direct laser interference ablation of GaN with a single pulse in each direction for different laser powers, and after cleaning with HCl. The pattern diameters

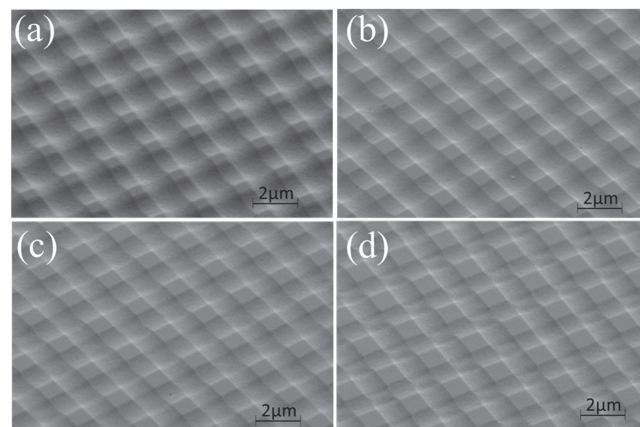


Figure 2. Direct laser interference ablation of GaN with different laser irradiation doses: a) 560 mJ cm⁻²; b) 382 mJ cm⁻²; c) 306 mJ cm⁻²; d) 153 mJ cm⁻². All pattern periods are 2.4 μm, pattern diameters are 5 mm.

are 5 mm, yielding input laser fluences of a) 560 mJ cm⁻²; b) 382 mJ cm⁻²; c) 306 mJ cm⁻²; and d) 153 mJ cm⁻². The laser irradiation causes the thermal decomposition of GaN into gaseous nitrogen and Ga droplets that remain on the surface and can be cleaned up by HCl.^[25] During laser interference patterning, the high-energy nanosecond laser selectively ablates the GaN surface. The resulting surface topography comprising a grid of flat mesas and V-shaped channels is an inverse of the corresponding laser intensity distribution. Both the height and the size of mesa can be controlled by the input laser fluence. The height increases with increasing exposure dose and follows the widely accepted form of Beer's law:

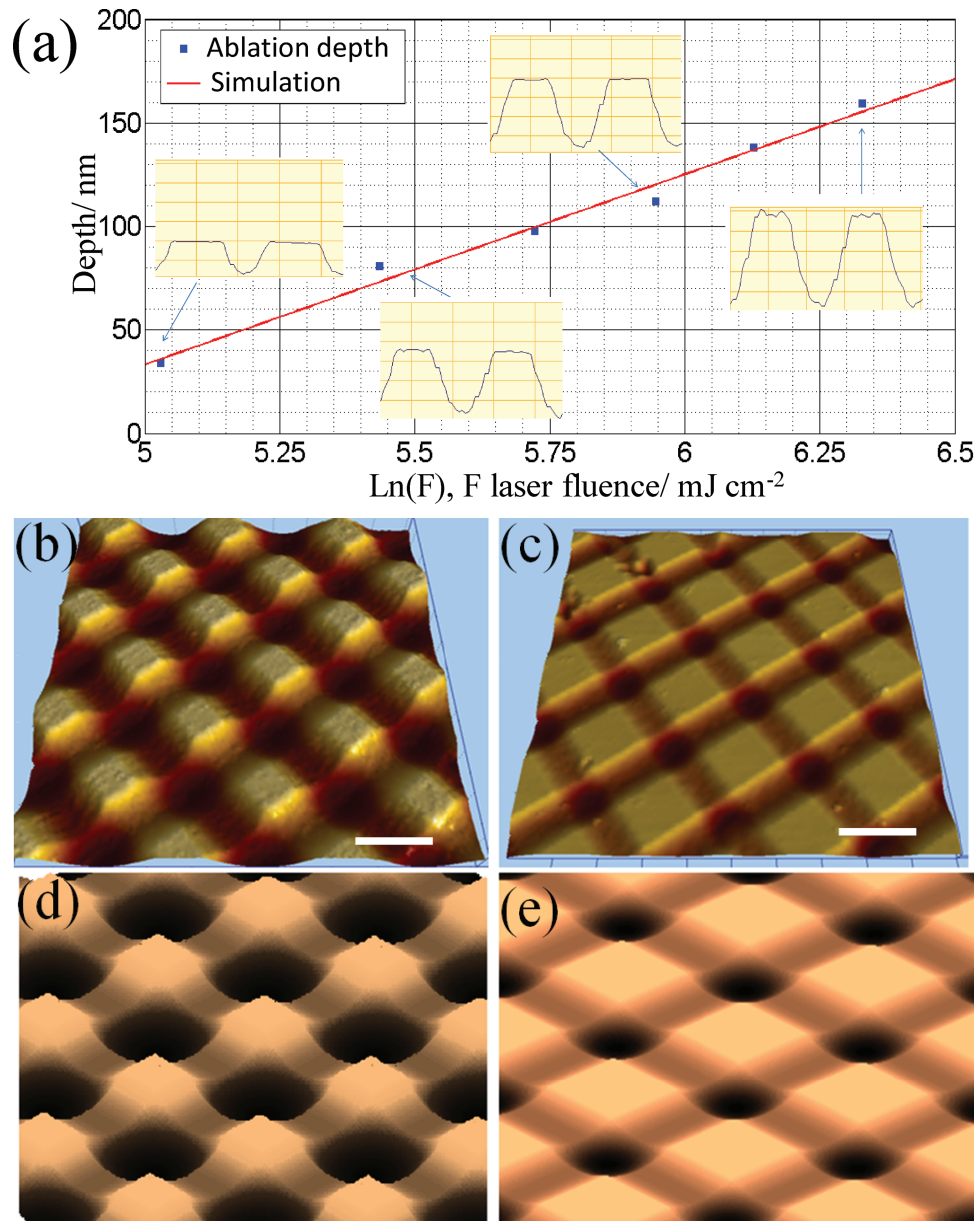


Figure 3. a) The ablation depth as a function of laser fluence. The insets are AFM profile images for representative data points; (b) and (c) the three-dimensional AFM images for the topographies of laser interference ablation of GaN with laser fluences 560 mJ cm⁻² and 126 mJ cm⁻², respectively. Pattern periods are 2.4 μm and patterns diameters are 5 mm, scale bars are 2 μm; (c) and (d) are computed topographies for (a) and (b), respectively.

$$d(F) = \frac{1}{\alpha_{\text{eff}}} \ln\left(\frac{F}{F_{\text{th}}}\right) \quad (2)$$

It represents the ablation depth or the height of the mesa (d) at various fluences (F), the threshold fluence (F_{th}), and the effective absorption coefficient (α_{eff}).^[25]

Atomic force microscopy (AFM) was used for topographic measurements (Veeco Dimension 3100) of the flat mesas ablated with different laser fluences. **Figure 3a** shows the ablation depth as a function of the logarithm of the laser fluence. Each data point was obtained by averaging the ablation depth over the whole measurement area (20 μm × 20 μm). The insets show four profiles of the patterned GaN

samples. Both the threshold fluence for ablation and the absorption coefficient for GaN at 266 nm can be achieved from the fit of the experimental data. The abscissa intercept corresponds to the threshold fluence, 103.5 mJ cm⁻². The absorption coefficient is obtained from the slope of the plot, and is 1.3×10^5 cm⁻¹. This value is in agreement with the reported data for GaN obtained from the optical measurement method.^[26–27]

The dependence of the size of the flat mesas on the laser fluence was also investigated. **Figure 3b** and **c** show representative topographies of laser interference ablation of GaN characterized through AFM. Tapping mode AFM was used

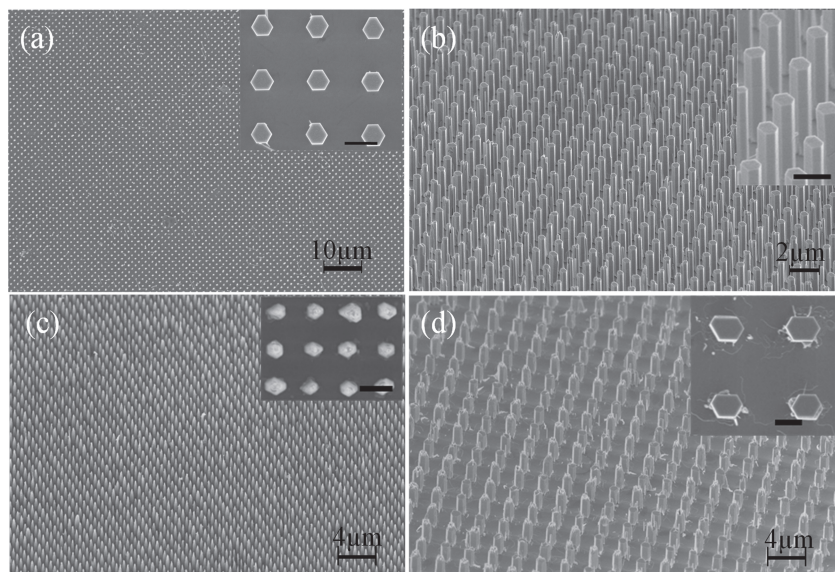


Figure 4. SEM images of vertically aligned ZnO nanowire arrays. a) Top and b) 45° tilted views of aligned individual ZnO nanowire arrays with uniform diameter, height and 2 μm period spanning centimeter-scale area. Insets are the enlarged images, scale bars are 1 μm ; (c) and (d) are ZnO nanowires grown on patterned GaN substrates with periods of 1 μm and 3 μm , respectively. Samples are tilted by 45°. Insets are enlarged SEM top views, scale bars are 1 μm .

for the measurement with the cantilever operating at a frequency of 244 kHz. The size of flat mesa increases with decreasing exposure dose. Figure 3d and e show the computed three-dimensional topographies for Figure 3b and c respectively, obtained by combining the laser intensity distribution (Equation 1), the Beer's law or ablation equation (Equation 2), and the threshold fluence and absorption coefficient from the experiments. The simulation results are in good agreement with the experimental data. Both experimental and simulation results confirmed that the size of the flat mesa can be controlled in the range of $P/5$ to approximately $4P/5$, where P is the interference period. The size of the flat mesas is a very important parameter influencing the size of the grown ZnO nanowires which will be discussed below.

Figure 4a and **b** show SEM images of aligned individual ZnO nanowire arrays with uniform diameter and height spanning an area of one 1 cm^2 . The insets show close-up images. The period is 2 μm and all ZnO nanowires grow on the flat mesas, which are the unablated areas of the GaN film. Before hydrothermal growth of ZnO nanowires, the average size of the flat mesas is around 630 nm. The average diameter of the ZnO nanowires after hydrothermal growth is 600 nm, which is slightly smaller than the flat mesas size.

Due to the flexibility of the laser interference ablation technique, the period and the pitch between nanowires can be varied in a relatively straightforward manner. Figure 4c and d show SEM images of ZnO nanowires grown on patterned GaN substrates with periods of c) 1 μm and d) 3 μm . All the pattern diameters here are 5 μm . However, enlarging the patterned area is possible through the integration of an x-y positioning stage into the LIA system.

Without using catalyst and without patterned photoresist, vertically aligned ZnO nanowire arrays were grown on top of

each GaN (0001) mesa patterned by LIA. It is seen clearly in Figure 4 that the pattern defined by LIA was preserved during the growth process. All of the ZnO nanowires grew perpendicular to the GaN substrate in a predefined pattern. In order to understand the ZnO nanowire growth mechanism and the interface structure, detailed structural characterizations of the LIA patterned GaN substrate were carried out using high resolution transmission electron microscopy (HRTEM) (JEOL 4000EX), shown in **Figure 5**. The cross-sectional image of the GaN substrate (Figure 5a) clearly demonstrates the flat GaN mesa and the valley produced by LIA. The flat GaN mesa is around 300 nm in size with a center-to-center spacing of 2.4 μm . Selected-area electron diffraction (SAED) patterns were taken with electron beam perpendicular to the flat GaN mesa. The surface structures of the GaN mesa (Figure 5b), sloping sides (Figure 5d), and bottom (Figure 5c) of the valley were studied with HRTEM. The GaN (0001) mesa is flat

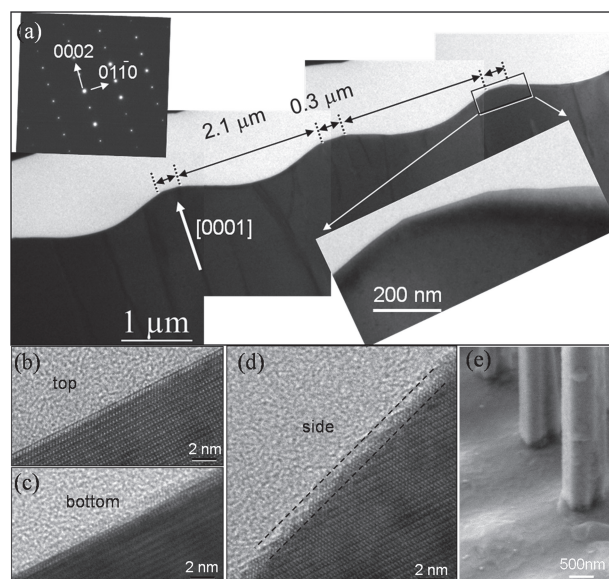


Figure 5. a) The cross-sectional image of the GaN substrate clearly demonstrates the flat GaN mesa and the valley produced by LIA. The flat GaN mesa is around 300 nm in size with a center-to-center spacing of 2.4 μm . Selected-area electron diffraction (SAED) pattern was taken with electron beam perpendicular to the flat GaN mesa. b–d) Surface structures of the GaN mesa: top (b) and sloping sides (d) of the mesas, and the bottoms (c) of the valleys were characterized by HRTEM. The GaN (0001) mesa is flat at the atomic level, which favors heteroepitaxial growth of ZnO nanowires along the c axis. The surfaces of the mesa sloping sides and the bottom of the valley have distortions, leading to changes in the lattice and possible suppression of the ZnO nanowires growth. e) Enlarged SEM image with 45° tilt of individual ZnO nanowires grown on patterned GaN substrate with 1 μm period, which shows ZnO nanowires prefer growing on the flat mesa surfaces.

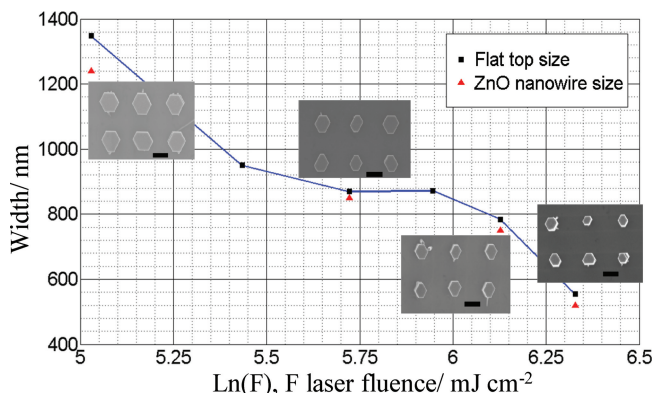


Figure 6. The relationship between the size of the flat mesas and the diameter of ZnO nanowires, under constant hydrothermal growth conditions. Insets are top view of SEM images of ZnO nanowires with period of 2.4 μm . Scale bars are 1 μm .

at the atomic level, which favors epitaxial growth of ZnO nanowires along the c axis. The surfaces of the mesa sloping sides and the bottoms of the valleys have distortions, leading to a change in the lattice and possible suppression of the ZnO nanowires growth on these surfaces. In order to achieve vertically aligned ZnO nanowire arrays, either by hydrothermal decomposition or physical vapor deposition method, matches in the crystallographic orientation and lattice parameter between the substrate material and ZnO are required. From the enlarged SEM image with 45° tilt of individual ZnO nanowires grown on patterned GaN substrate with 1 μm period, Figure 5e, it can be seen that ZnO nanowires prefer growing on the flat mesa surfaces.

The shape of ZnO nanowires can be tuned by hydrothermal growth parameters such as solution concentration, growth temperature and time. Given the same growth condition, the sizes of the flat mesas also play a very important role in controlling the size of grown ZnO nanowires. **Figure 6** shows the relationship between the size of flat mesas and the diameter of ZnO nanowires. All of the patterns were fabricated on different regions of the same GaN substrate, and the ZnO nanowires were then grown in the same solution and under the same conditions. The square symbols are the sizes of the flat mesas while the triangle symbols are the sizes of the ZnO nanowires. The plot illustrates proportionality between sizes of ZnO nanowires and the flat mesas accordingly.

4. Conclusions

In summary, we have developed a method to produce periodic individual ZnO nanowires on GaN over areas spanning one square-centimeter by combining LIA and hydrothermal method. Simulation of LIA of GaN was conducted, which showed good agreement with the experimental data. We have demonstrated the highly controlled and uniform growth of ZnO nanowire arrays with different sizes and periods, proving high application potential for sensor arrays, piezoelectric devices, and optoelectronic devices.

5. Experimental Section

Laser Interference Ablation: A commercial Nd:YAG laser (Quanta-Ray PRO 290, Spectra Physics) emitting a 10 mm diameter beam was used in the laser interference lithography experiments. The fundamental wavelength of the Nd:YAG laser is 1064 nm from which shorter wavelengths (532 nm, 355 nm and 266 nm) can be obtained by harmonic generation. For our experiments, samples were irradiated with 10 ns pulses of 266 nm wavelength at a repetition rate of 10 Hz. Figure S1 shows a schematic of the laser interference lithography setup. The P-polarized laser beam is split into two beams by a 50/50 beam splitter (5) and then recombined at a rotation stage (9) for holding samples with a designed interference angle (θ).

In the experiment, periodic line-like patterns on the GaN surface were first generated through the interference of two 266 nm laser beams. The sample was then turned by 90 degrees and patterned with a second line-like pattern. The intensity distribution after the two exposures is shown in figure S2. An iris diaphragm was installed in front of the samples to reduce the exposure area from 10 to 5 mm in diameter so as to achieve uniform fluence over the entire patterned area.

The laser power can be adjusted through the controller of the laser and is monitored by a high damage threshold power meter (2) together with a 10% reflection beam splitter (5). An electromechanical shutter (3) (Uniblitz Electronic VS25S2ZMO, 3.0 ms temporal resolution) controls the exposure time. The samples are loaded on the precision rotation stage and exposed to the pulsed interference pattern. All the experiments are performed in an ambient atmosphere environment.

Hydrothermal Growth of ZnO Nanowires: The growth of ZnO nanowires was conducted in a convection box oven (Yamato). The patterned GaN substrates were faced down and suspended on the surface of a mixture of equal molar aqueous solutions of zinc nitrate (Alfa Aesar) and hexamethylenetetramine (HMTA) (Fluka) in an airproof container. The container was then placed in the convection box oven at 85 $^\circ\text{C}$ for 24 h. Vertical alignment of ZnO nanowires was achieved due to the small lattice mismatch between the GaN substrate plane and the ZnO plane.

Acknowledgements

D. Yuan and R. Guo contributed equally to this work. Research was supported by the Georgia Institute of Technology, DARPA (Army/AMCOM/REDSTONE AR, W31P4Q-08-1-0009), BES DOE (DE-FG02-07ER46394), KAUST Global Research Partnership, NSF (DMS0706436, CMMI 0403671), and the MANA WPI program from NIMS, Japan.

Received: May 25, 2010

Published online:

- [1] Z. W. Pan, Z. R. Dai, Z. L. Wang. *Science* **2001**, 291, 1947.
- [2] M. H. Huang, Y. Wu, H. Feick, N. Tran, E. Weber, P. Yang. *Science* **1997**, 277, 1978.
- [3] X. Wang, C. J. Summers, Z. L. Wang. *Nano Lett.* **2004**, 4, 423.
- [4] X. Y. Kong, Z. L. Wang. *Nano Lett.* **2003**, 3, 1625.
- [5] X. Wang, J. Song, J. Liu, Z. L. Wang. *Science* **2007**, 316, 102.
- [6] Z. L. Wang, J. Song. *Science* **2006**, 312, 242.
- [7] M. S. Arnold, P. Avouris, Z. W. Pan, Z. L. Wang. *J. Phys. Chem. B* **2003**, 107, 659.
- [8] M. Law, L. E. Greene, J. C. Johnson, R. Saykally, P. Yang. *Nat. Mater.* **2005**, 4, 455.
- [9] H. Yan, R. He, J. Johnson, M. Law, R. J. Saykally, P. Yang. *J. Am. Chem. Soc.* **2003**, 125, 4728.
- [10] C. H. Liu, J. A. Zapien, Y. Yao, X. M. Meng, C. S. Lee, S. S. Fan, Y. Lifshitz, S. T. Lee. *Adv. Mater.* **2003**, 15, 838.

- [11] J. B. Cui, C. P. Daghljan, U. J. Gibson, R. Pusche, P. Geithner, L. Ley. *J. Appl. Phys.* **2005**, *97*, 044315.
- [12] N. Saito, H. Haneda, T. Sekiguchi, N. Ohashi, I. Sakaguchi, K. Koumoto. *Adv. Mater.* **2002**, *14*, 418.
- [13] Z. Zhong, D. Wang, Y. Cui, M. W. Bockrath, C. M. Lieber. *Science* **2003**, *302*, 1377.
- [14] S. Xu, Y. Wei, M. Kirkham, J. Liu, W. Mai, D. Davidovic, R. L. Snyder, Z. L. Wang. *J. Am. Chem. Soc.* **2008**, *130*, 14958.
- [15] J. Rybczynski, D. Banerjee, A. Kosiorek, M. Giersig, Z. F. Ren. *Nano Lett.* **2004**, *4*, 2037.
- [16] H. J. Fan, B. Fuhrmann, R. Scholz, F. Syrowatka, A. Dadgar, A. Krost, M. Zacharias. *J. Cryst. Growth* **2006**, *287*, 34.
- [17] A. I. Hochbaum, R. Fan, R. He, P. Yang. *Nano Lett.* **2005**, *5*, 457.
- [18] T. Martensson, P. Carlberg, M. Borgstrom, L. Montelius, W. Seifert, L. Samuelson. *Nano Lett.* **2004**, *4*, 699.
- [19] T. C. Chong, M. H. Hong, L. P. Shi. *Laser Photon. Rev.* **2010**, *4*, 123.
- [20] Y. Wei, W. Wu, R. Guo, D. Yuan, S. Das, Z. L. Wang. *Nano Lett.*, in press.
- [21] J. Zhang, L. Sun, J. Yin, H. Su, C. Liao, C. Yan. *Chem. Mater.* **2002**, *14*, 4172.
- [22] L. E. Greene, B. D. Yuhas, M. Law, D. Zitoun, P. Yang. *Inorg. Chem.* **2006**, *45*, 7535.
- [23] Y. Wei, Y. Ding, C. Li, S. Xu, J. H. Ryo, R. Dupuis, A. K. Sood, D. L. Polla, Z. L. Wang. *J. Phys. Chem. C* **2008**, *112*, 18935.
- [24] X. Wang, J. Song, C. J. Summers, J. H. Ryou, P. Li, R. D. Dupuis, Z. L. Wang. *J. Phys. Chem. B* **2006**, *110*, 7720.
- [25] C. F. Chu, F. I. Lai, J. T. Chu, C. C. Yu, C. F. Lin, H. C. Kuo, S. C. Wang. *J. Appl. Phys.* **2004**, *95*, 3916.
- [26] G. D. Chern, H. E. Tureci, A. D. Stone, R. K. Chang, M. Kneissl, N. M. Johnson. *Appl. Phys. Lett.* **2003**, *83*, 1710.
- [27] J. F. Muth, J. H. Lee, I. K. Shmagin, R. M. Kolbas, H. C. Casey Jr, B. P. Keller, U. K. Mishra, S. P. DenBaars. *Appl. Phys. Lett.* **1997**, *71*, 2572.